Structural basis for substrate specificity of an amino acid ABC transporter

Jie Yu[a,1], Jingpeng Ge[a,1], Johanna Heuveling[b], Erwin Schneider[b,2], and Maojun Yang[a,2]

[a]Ministry of Education Key Laboratory of Protein Sciences, Tsinghua-Peking Center for Life Sciences, School of Life Sciences, Tsinghua University, Beijing 100084, China and [b]Division of Microbial Physiology, Department of Biology, Humboldt University of Berlin, D-10099 Berlin, Germany

Edited* by Douglas C Rees, Howard Hughes Medical Institute, Caltech, Pasadena, CA, and approved March 6, 2015 (received for review August 6, 2014)

ATP-binding cassette (ABC) transporters are ubiquitous integral membrane proteins that translocate a variety of substrates, ranging from ions to macromolecules, either out of or into the cytosol (hence defined as importers or exporters, respectively). It has been demonstrated that ABC exporters and importers function through a common mechanism involving conformational switches between inward-facing and outward-facing states; however, the mechanism underlying their functions, particularly substrate recognition, remains elusive. Here we report the structures of an amino acid ABC importer Art(QN)$_2$ from *Thermoanaerobacter tengcongensis* composed of homodimers each of the transmembrane domain ArtQ and the nucleotide-binding domain ArtN, either in its apo form or in complex with substrates (Arg, His) and/or ATPs. The structures reveal that the straddling of the TMDs around the twofold axis forms a substrate translocation pathway across the membrane. Interestingly, each TMD has a negatively charged pocket that together create a negatively charged internal tunnel allowing amino acids carrying positively charged groups to pass through. Our structural and functional studies provide a better understanding of how ABC transporters select and translocate their substrates.

ABC transporters | substrate selectivity | inward-facing state | two binding sites | type I importer

ATP-binding cassette (ABC) transporters represent one of the most abundant protein superfamilies in both prokaryotes and eukaryotes (1, 2). Powered by ATP hydrolysis, ABC transporters mediate translocation of a vast variety of molecules, ranging from ions to proteins, across membranes, and participate in the regulation of many cellular processes (3, 4). Depending on the direction of substrate flux, ABC transporters can be subdivided into importers and exporters (5). Minimal ABC transporters consist of two transmembrane domains (TMDs) in complex with two nucleotide-binding domains (NBDs). Canonical ABC importers found in prokaryotes also require the assistance of extracellular (or periplasmic) solute-binding proteins (SBPs) to transport substrates from the exterior to the cytoplasm, such as what is observed in the maltose transporter MalFGK$_2$ (6).

To date, structures of several ABC transporters, including entire functional complexes and separately expressed NBDs, have been reported (7–17). As a general architecture, the straddling of two TMDs creates the translocation pathway across the membrane. The NBDs, which bind and hydrolyze ATP, comprise a highly conserved RecA-like subdomain containing Walker A and B motifs and a helical subdomain containing the LSGGQ signature motif (18, 19). Structural and biological studies have demonstrated that ABC transporters may function through a mechanism involving switching of the translocation path between an inward-facing and an outward-facing conformation, a process termed the "alternate access" mode. Conformational changes leading to these alternate states seem to differ among transporter subtypes, however (20, 21).

In this paper, we report crystal structures of an ABC importer for positively charged amino acids, Art(QN)$_2$, from the thermophilic bacterium *Thermoanaerobacter tengcongensis* in its apo form, as well as in complex with Arg, His, and/or ATP at 2.8-, 2.6-, 2.8-, 3-, and 2.5-Å resolution, respectively. In addition, we solved the structure of the cognate SBP, ArtI, in complex with Arg at 1.48 Å. Together with functional analyses, we are able to reveal an evolutionarily conserved mechanism underlying the substrate selectivity of ABC transporters.

Results and Discussion

Functional Characterization of the ArtI-Art(QN)$_2$ Complex. Most canonical ABC import systems display low spontaneous ATPase activity that is stimulated by their cognate SBP liganded with the respective substrate. With the exception of the maltose transporter of *Escherichia coli*/*Salmonella*, this is usually observed in a lipid environment, but not in detergent solution (22–25). Because insufficient amounts of *T. tengcongensis* cells for the extraction of lipids were available to us, we performed reconstitution of Art(QN)$_2$ with phospholipids from the thermophilic bacterium *Geobacillus stearothermophilus*, which grows at a similar ambient temperature as *T. tengcongensis* (60–70 °C). Proteoliposomes prepared from the Arg/His/Lys transporter ArtJ-(MP)$_2$ and lipids of *G. stearothermophilus* were recently demonstrated to exhibit SBP-stimulated ATPase and transport activity (26).

To our knowledge, this is the only report to date on such activities of a multisubunit ABC transporter from a thermophilic organism. We reasoned that *G. stearothermophilus* lipids might be suited for verifying the functionality of the ArtI-(QN)$_2$ system, even though optimal activities might not be obtained. Guided by predictions from sequence alignments, ArtI-stimulated ATPase

Significance

Here we report the crystal structures of an amino acid ATP-binding cassette (ABC) importer either in its apo form or in complex with substrates (Arg, His) and/or ATPs. Interestingly, each transmembrane domain has a negatively charged pocket, allowing amino acids carrying positively charged groups to pass through. Functional analyses of the transporter in proteoliposomes indicate its capability to undergo substrate-dependent conformational changes resulting in stimulated ATPase activity. Taken together, we identified a previously undefined substrate binding mode of ABC transporters and shed light on the mechanism underlying how ABC transporters select and translocate their substrates.

Author contributions: J.Y., J.G., J.H., E.S., and M.Y. designed research; J.Y., J.G., and J.H. performed research; J.Y., J.G., J.H., E.S., and M.Y. analyzed data; and J.Y., J.G., E.S., and M.Y. wrote the paper.

The authors declare no conflict of interest.

*This Direct Submission article had a prearranged editor.

Freely available online through the PNAS open access option.

Data deposition: The crystallography, atomic coordinates, and structure factors have been deposited in the Protein Data Bank, www.pdb.org (PDB ID codes 4YMS, 4YMT, 4YMU, 4YMV, 4YMW, and 4YMX).

[1]J.Y. and J.G. contributed equally to this work.

[2]To whom correspondence may be addressed. Email: erwin.schneider@rz.hu-berlin.de or maojunyang@tsinghua.edu.cn.

This article contains supporting information online at www.pnas.org/lookup/suppl/doi:10.1073/pnas.1415037112/-/DCSupplemental.

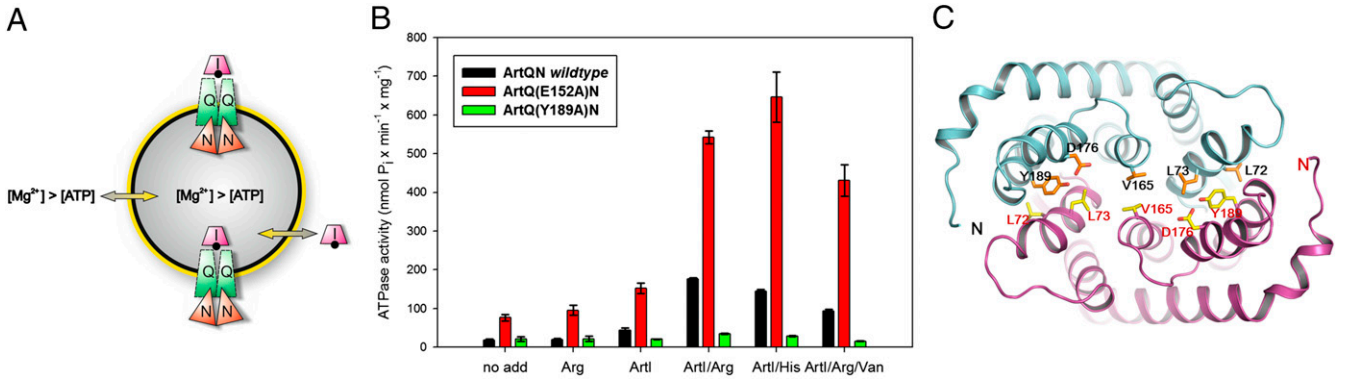

Fig. 1. Liganded ArtI stimulates the ATPase activity of Art(QN)$_2$. (*A*) Cartoon illustrating the experimental setup of the ATPase assay. Art(QN)$_2$ is incorporated into proteoliposomes in two possible orientations: with the nucleotide-binding subunits, ArtN$_2$, facing the medium or being exposed to the lumen of the proteoliposomes. ATPase activity is initiated by adding ArtI, Arg/His (black dot), ATP, and Mg^{2+} ions (in excess over ATP). Under these conditions, Mg^{2+} will permeabilize the proteoliposomes (24), thus allowing access of ATP and ArtI/Arg/His to the lumen. (*B*) Purified variants were incorporated into liposomes formed from *G. stearothermophilus* lipids and assayed for ATPase activity in the presence or absence of ArtI/Arg or ArtI/His. Reactions were started by adding 3 mM $MgCl_2$ and 2 mM ATP to preheated (70 °C) proteoliposomes in the presence of 50 mM Mops (pH 7.5), ArtI (35 μM), L-arginine or L-histidine (100 μM each), and *ortho*-vanadate (1 mM) (where indicated). Aliquots (25 μL containing 3 μg of protein) were taken in 2-min intervals and placed into wells of a microtiter plate containing 25 μL of a 12% (wt/vol) SDS solution. The amount of liberated phosphate was determined colorimetrically with ammonium molybdate complexes using Na_2HPO_4 as the standard. Further details are provided in *SI Methods*. SE mean ($n \geq 3$). (*C*) Ribbon diagram of TM helices surrounding with substrate-binding sites viewed along the membrane bilayer from the periplasmic side. ArtQ subunits are colored in cyan and magenta. The residues involved in dimer formation of ArtQ are shown in ball-and-stick models.

activity of Art(QN)$_2$ in proteoliposomes was monitored in the presence of either Arg or His (Fig. 1*A*). As shown in Fig. 1*B*, proteoliposomes containing Art(QN)$_2$ exhibited low ATPase activity at 70 °C that was slightly increased in the presence of ArtI alone. In contrast, the addition of Arg- or His-loaded ArtI resulted in approximately fourfold stimulation of the rate of ATP hydrolysis (Fig. 1*B*), similar to what was observed for the closely related ArtJ-(MP)$_2$ transporter (26). Moreover, the ATPase activity was demonstrated to be sensitive to *ortho*-vanadate, a specific inhibitor of ABC-type ATPases in the context of the complete transporter (27), albeit to a lesser degree than reported for other ABC import systems (Fig. 1*B*).

In contrast, transport assays basically performed under conditions that resulted in uptake of radiolabeled Arg in the case of the ArtJ-(MP)$_2$ transporter of *G. stearothermophilus* were unsuccessful (26). However, whereas the Art(MP)$_2$ complex was assayed at 55 °C, Art(QN)$_2$ had to be measured at 70 °C owing to a substantial drop in ATPase activity already at 60 °C (below 50% of the control). Because 70 °C is at the upper temperature limit at which *G. stearothermophilus* can grow, it appears plausible that at this temperature, proteoliposomes prepared from the homemade lipids of the organism are less stable ("leaky"), thereby preventing accumulation of transported substrate in the lumen. At first glance, this notion seems to contradict the results of ATPase measurements, which were also performed at 70 °C; however, although intact proteoliposomes are a prerequisite for transport assays, stimulation of ATPase activity by substrate-loaded binding protein requires only a lipid environment, as indicated by reports demonstrating stimulation in lipid nanodiscs, a phospholipid bilayer stabilized by two copies of an amphipathic membrane scaffold protein that wraps around the periphery of the bilayer (28, 29).

Because the lipid composition of *T. tengcongensis* is not known, we cannot exclude the possibility that coupling of ArtI/Arg-stimulated ATPase activity of Art(QN)$_2$ to transport in an in vitro system might require one or more components from the native lipid membrane. As recently shown for the maltose ABC transporter, the lipid composition of the membrane can indeed affect coupling of ATPase activity to transport (28).

We emphasize that functional reconstitution and transport assays performed with multisubunit transporters from thermophilic or hyperthermophilic organisms are not yet established procedures, owing mainly to the lack of high-quality lipids from such organisms. Therefore, we could test the functionality of the ArtI-(QN)$_2$ system only under suboptimal conditions. Nonetheless, demonstrating substrate-dependent stimulation of ATPase activity of Art(QN)$_2$ in a lipid environment is considered evidence in favor of a functional canonical prokaryotic ABC import system with specificity for positively charged amino acids.

Overall Structure of ArtI. To further understand the determinants of substrate specificity of the ArtI-Art(QN)$_2$ complex, we first solved the crystal structure of ArtI complexed with Arg at 1.48 Å (Fig. 2*A* and Fig. S1*A*). Similar to other SBPs, ArtI is folded into two distinct domains (lobes) connected by a hinge composed of two loop segments (30–33) (Fig. 2*A*). Lobe I contains three β-sheets and three α-helices, whereas lobe II contains a central core of a five-stranded parallel β-sheet surrounded by α-helices (31). The interface between the two lobes forms the substrate-binding pocket that traps Arg deeply within ArtI. The ArtI^{Ser44}, ArtI^{Asp46}, ArtI^{Glu51}, ArtI^{Ala105}, ArtI^{Arg113}, ArtI^{Gly106}, ArtI^{Met107}, ArtI^{Glu193}, and ArtI^{Thr156} residues are engaged in hydrogen bonds and van der Waals interactions with the positively charged side chain of Arg (Fig. 2*B*). Sequence alignment shows that these residues are also highly conserved among ArtI homologs from various species (Fig. S2). Structural comparison with the Arg-, His-, and Lys-binding protein ArtJ of the ArtJ-(MP)$_2$ transporter from *G. stearothermophilus* (31) suggests that ArtI may also bind Lys and His, which in the latter case was subsequently proven experimentally (Fig. 2*C* and Fig. S3). Results from isothermal titration calorimetry (ITC) show that ArtI binds Arg with an apparent K_d of 79 nM (Fig. S3*A*), which is in the range of values reported for related SBPs (30–32). His also binds to ArtI, albeit with an unusually high apparent K_d of 176 μM (Fig. S3*B*). Nonetheless, binding of His is considered specific, because no interaction of ArtI with either glutamate (negatively charged) or threonine (polar, uncharged) could be detected (Fig. S3*B*). Taken together, these data indicate that ArtI displays binding affinities for both positively charged amino acids, consistent with ATPase measurements (Fig. 1*B*), but with a clear preference for Arg.

Overall Structure of the Art(QN)$_2$ Complex. In all structures obtained, an Art(QN)$_2$ dimer formed by two copies each of ArtQ and

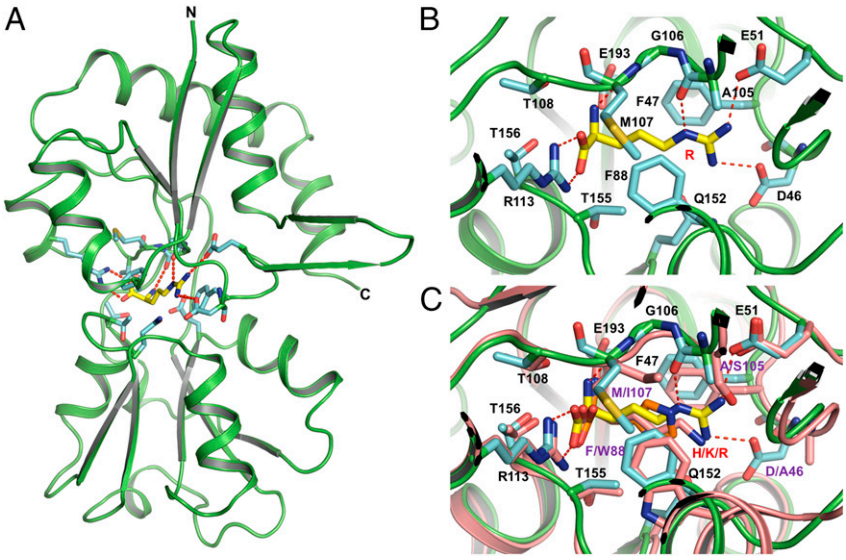

Fig. 2. Overview structure of the substrate-binding protein ArtI complexed with Arg. (*A*) ArtI is colored in green. The residues represented in cyan sticks interact with Arg mostly through hydrogen bonds and van der Waals force. Arg is shown in ball-and-stick models. Hydrogen bonds are represented as red dashed lines. (*B*) Stereoview of a detailed ribbon diagram of the Arg binding site of ArtI. Representative models of the residues from the substrate binding site as well as Arg are the same as in *A*; hydrogen bonds are represented as red dashed lines. (*C*) Stereoview of the structural alignment between ArtI and ArtJ of the ArtJ-$(MP)_2$ transporter from *G. stearothermophilus* (PDB ID codes 2Q2A, 2PVU, and 2Q2C). ArtI and ArtJ are colored in green and pink, respectively. Lys, Arg, and His are shown in ball-and-stick models. In ArtJ, residues that mediate substrate binding are shown in pink sticks.

ArtN was present, adopting an inward-facing conformation with the TMDs open to the cytoplasm (Fig. 3*A*). Each pair of ArtQ or ArtN subunits is closely related to an exact twofold axis passing through the center of the transporter. Similar to transmembrane components of type I ABC importers (34), ArtQ has five transmembrane segments (TMs). TM1 wraps around the outer membrane-facing surface and makes contact with the other four TM helices, which adopt an "up-down" topology that lines the translocation pathway. The structure of ArtQ shows a similar fold as MetI of the methionine uptake system of *E. coli* (9). The rmsd between ArtQ and MetI is approximately 2.6 Å with 269 Cα atoms aligned (Fig. 3*B*). Two ArtQ subunits are packed together in the membrane inner leaflet to expose the substrate-binding sites to the cytoplasm (Fig. 3*A*). Correct dimer formation is crucial for function, as revealed by analysis of a transporter variant containing ArtQ-Y189A that displayed complete loss of ATPase activity (Fig. 1). In addition, ArtN subunits interact with ArtQ primarily through the EAA motif [EAA-X(3)-G] of the TM subunits that have been identified previously (35, 36) (Fig. 3*B*).

Each ArtQ Subunit Contains One Substrate-Binding Site. Unlike the maltose ABC transporter, the only other ABC importer for which a substrate-binding site within the transmembrane domains is known (13), the Art$(QN)_2$ complex contains two substrate-binding sites; i.e., two Arg or His are bound at the interface between two ArtQ subunits, reaching halfway across the predicted membrane bilayer from the periplasmic surface (Figs. S1 *B* and *C* and S4*A*). In the structure with Arg, TM2, TM3, and TM4 of ArtQ contribute to binding of the substrate (Fig. 4*A*). $ArtQ^{Glu152}$ interacts directly with the guanidine group of Arg by forming salt bridges. In addition, hydrogen bonding and van der Waals interactions between Arg and $ArtQ^{Pro66}$, $ArtQ^{Asn98}$, $ArtQ^{Leu67}$, $ArtQ^{Val155}$, $ArtQ^{Met156}$, and $ArtQ^{Glu159}$, and especially pairing of the guanidine group with the benzene ring of $ArtQ^{Tyr102}$, further stabilize substrate binding (Fig. 4*A*). Binding of His to Art$(QN)_2$ is similar, involving the same residues as in binding Arg (Fig. 4*A*). These residues form two highly negatively charged electrostatic potential pockets (Fig. 4*C*). His and Arg both have a large positively charged group that can bind to the substrate-binding pocket (Fig. 4*A*). Notably, crystallization of Art$(QN)_2$ in the presence of

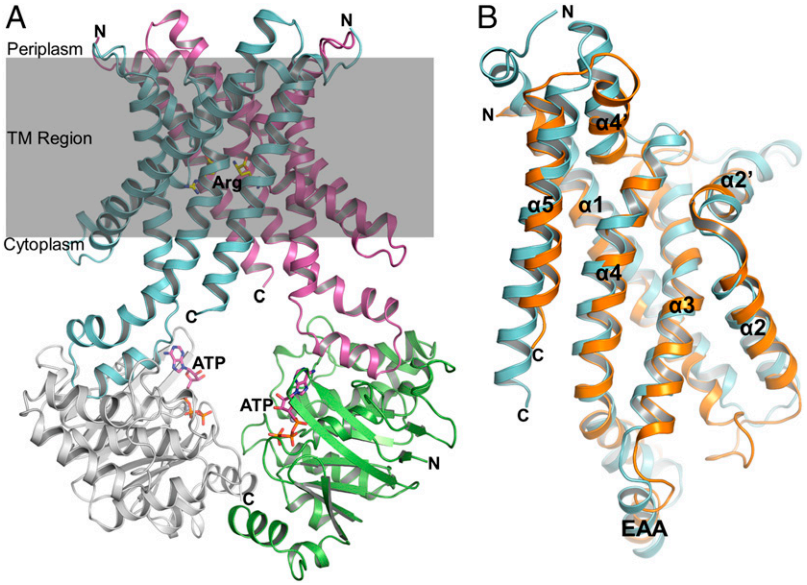

Fig. 3. Overview structure of the Art$(QN)_2$ complex in an inward-facing conformation. (*A*) Two transmembrane subunits (ArtQ) are colored in cyan and magenta, and two nucleotide-binding subunits (ArtN) are colored in gray and green. Arg and ATP molecules are shown in ball-and-stick models. (*B*) Stereo views of the structural alignment between ArtQ and MetI of the methionine uptake system Met$(NI)_2$ of *Escherichia coli* (PDB ID code 3DHW). MetI and ArtQ are colored in orange and cyan, respectively.

both Arg and His, only resulted in structures with two bound Arg. Although speculative, this might indicate that, as in ArtI, the binding sites have different affinities for the substrates.

Sequence alignment of ArtQ homologs from different species revealed that ArtQ^{P66}, ArtQ^{L67}, ArtQ^{N98}, ArtQ^{Y102}, ArtQ^{E152}, ArtQ^{E159}, ArtQ^{V155}, and ArtQ^{M156} residues involved in substrate interaction are highly conserved, suggesting the possibility that Art$(QN)_2$ homologs may share a common mechanism to determine substrate specificity (Fig. S5). To further strengthen this notion, we modeled HisM/HisQ, the TMDs of the well-characterized (heterodimeric) His-, Lys-, and Arg-transporter from *Salmonella enterica* serovar Typhimurium, separately into ArtQ (Fig. S6) (37–39). Results from sequence and structural alignments suggest that substrate-binding sites are highly conserved except for Glu159 (Ser in HisM, Ala in HisQ), Met156 (Ile in HisQ), Asn98 (Ile in HisQ), and K158 (His in HisM) (Figs. S5 and S6).

To further explore the role of these residues in coordinating the substrate within the TMDs, we have investigated the functional consequences of mutating ArtQ-E152 to Ala. Unexpectedly, both basal level and ArtI/Arg/His-stimulated ATPase activity of the variant in proteoliposomes were substantially increased compared with wild type (Fig. 1). Apparently, the mutation changes the binding pocket such that ATP hydrolysis at the ArtN dimer is triggered even in the absence of substrate. In contrast, and like the wild-type transporter, ATPase activity was stimulated approximately fourfold by substrate, whereas vanadate sensitivity was lower. Interestingly, this finding is reminiscent of the phenotype of mutations affecting the highly conserved residue ArtM-K159 (K158 in ArtQ) of the Art$(MP)_2$ transporter of *G. stearothermophilus*, which also resulted in a substantial increase in ATPase activity, albeit uncoupled from transport (26). Taken together, the results of our mutational analysis underscore the crucial role of ArtQ^{E152} within the binding pocket as indicated by the structural data.

No obvious conformational changes were observed comparing the structures in apo-bound and Arg-bound states, although the residues interacting with the substrate displays slight changes (Fig. 4*B*). When the substrate binds to ArtQ, the substrate binding pockets pack more tightly than in the apo state (Fig. 4 *C* and *D*).

Common Features of Substrate Specificity. Structural analyses suggest that each ArtQ molecule contains a highly negatively charged electrostatic potential tunnel reaching from the extracellular side to the cytoplasmic side, in which a highly negatively charged substrate-binding pocket lies in the middle of the protein (Fig. 5*A*). This internal negatively charged tunnel could permit amino acids carrying a positively charged side chain, such as Arg or His, to pass through. Indeed, the positively charged head groups of Arg or His are inserted into the pockets (Fig. 5*A*). Although the overall structure of ArtQ is very similar to that of MetI in *E. coli*, the residues that participate in substrate binding are highly diverse (9) (Fig. 5*B*). Genomic analyses with putative amino acid transporters from different species suggest that the residues corresponding to ArtQ^{P66} and ArtQ^{Y102} are highly conserved (Table 1). This is consistent with our structural observation that the main chain of ArtQ^{P66} and the benzene ring of ArtQ^{Tyr102} are generally important for binding amino acid substrates (Fig. 4*A*), whereas the other residues might be responsible for recognizing the specificity of the substrates.

Inward-Facing State with Substrates and ATPs. Unlike the MetN protein from the methionine uptake system that contains a C-terminal extension at which the transporter's activity is regulated by internal methionine, ArtN lacks such a feature. Two ArtN subunits pack together, and the Walker A and Walker B motifs

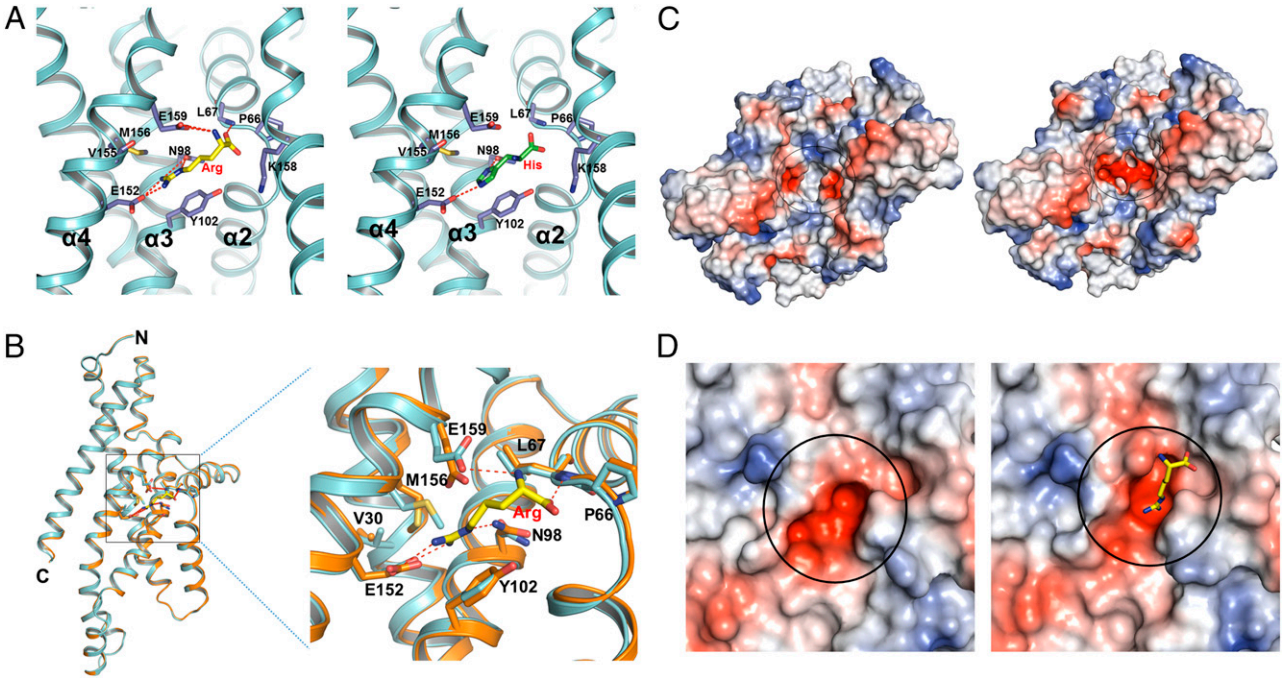

Fig. 4. Comparison of conformational changes of the substrate-binding site in the apo-bound and Arg-bound states. (*A*) Stereo views of the Arg (*Left*) and His (*Right*) binding site, with hydrogen bonds indicated by red dashed lines. ArtQ is colored in cyan; Arg and His are shown in yellow and green sticks, respectively; and residues interacting with substrate are shown as blue sticks. (*B*) Relative positions of the residues in the substrate-binding site (indicated by a black square) display slight changes by superposition of the two ArtQ subunits in different states. Apo-bound and Arg-bound ArtQ subunits are colored in yellow and cyan, respectively. Arg is shown in ball-and-stick models. Hydrogen bonds are represented as red dashed lines. (*C*) Comparison of overall electrostatic potential surface of the substrate-binding site (indicated by a black circle) between apo-bound (*Left*) and Arg-bound (*Right*) states. Representative model of Arg is as in *A*. (*D*) Close-up of the electrostatic potential surface of the substrate-binding site of apo-bound (*Left*) and Arg-bound (*Right*) states.

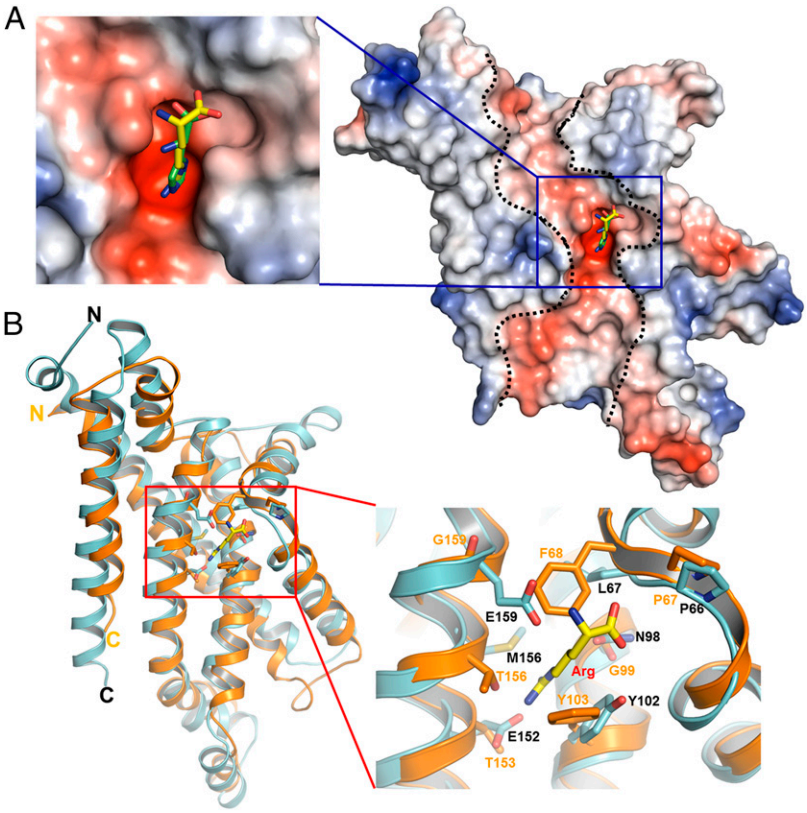

Fig. 5. A highly negatively charged substrate binding pocket lies in the middle of the protein. (*A*) ArtQ contains a highly negatively charged electrostatic potential tunnel (indicated by dashed lines) reaching from the periplasmic side to the cytoplasmic side. A highly negatively charged substrate-binding pocket, indicated by a blue square, lies in the middle of the protein. Arg is shown in ball-and-stick representation. (*B*) Stereo views of the structural alignment of the substrate-binding site of ArtQ with the corresponding region of MetI of the methionine uptake system $Met(NI)_2$ from *E. coli* (PDB ID code 3DHW). MetI and ArtQ dimers are colored in orange and cyan, respectively. The residues interacting with substrate as well as Arg are shown in ball-and-stick models.

from one monomer lie opposite to the LSGGQ motif of the other in a "head-to-tail" manner, as has been observed in the structures of other ABC transporters as well (7–15, 40) (Fig. S4*B*). Although the two ArtN subunits are modestly separated, two ATP molecules are bound at Walker A and Walker B motifs of each subunit, respectively (Fig. 3*A* and Fig. S4*C*). Compared with other NBD subunits of ABC transporters, arrangement of the two ArtN subunits most closely resembles the "semi-open" form of the MalK dimer. The alignment of the ArtN dimer with open or semi-open states of the MalK dimer revealed rmsd values of 3.8 Å and 2.8 Å, respectively (10, 12) (Fig. S7). Thus, the structure represents an inward-facing conformation of the ArtQ dimer but with the ArtN subunits residing in a semi-open state.

We also solved the structure of $Art(QN)_2$ in complex with both Arg and ATP (Fig. 3*A*). Interestingly, no obvious conformational changes were found among apo-, ATP-, Arg-, and Arg/ATP-bound forms. The rmsd values among these structures are less than 0.2 Å (Fig. S8). Previous studies suggested that ATP binding to the NBD subunits would induce an overall structural change from the inward-facing state to the outward-facing state (5, 41); however, for ABC importers, the vast preponderance of structural, biochemical, and biophysical evidence indicates that this conformational switch also requires the presence of the binding protein (20, 29). Consistently, ArtI, liganded with Arg or His, could stimulate the ATPase activity of the $Art(QN)_2$ complex (Fig. 1*A*). Thus, the lack of ArtI in our crystallization trials provides a likely explanation for our finding. Unfortunately, thus far attempts to obtain crystal structures of $Art(QN)_2$ in complex with ArtI have not been successful.

Conclusions

In the present study, we determined the crystal structures of the Art $(QN)_2$ transporter in its apo state as well as in complex with substrates (Arg, His) and/or ATP. In the absence of the cognate binding protein ArtI, all structures reveal that the transporter was captured in an inward-facing semi-open conformation. Crystal structures of $Art(QN)_2$ with bound ArtI could not be obtained; nonetheless, functional analyses of the transporter in proteoliposomes indicate its capability to undergo substrate-dependent conformational changes resulting in stimulated ATPase activity.

Table 1. Residues that mediate substrate binding from the proposed different amino acid transporters

Transporter	Sample no.	Position					
		P66	L67	N98	Y102	E152	E159
Arginine	20	P 20	L 14 E 5 M 1	N 15 I 5	Y 20	E 15 L 5	E 12 D 6 A/G 1
Histidine	49	P 49	L 48 M 1	N 49	Y 49	E 49	S 27 A 16 G 5 T 1
Ectoine/ hydroxyectoine	29	P 29	L 26 I 3	H 25 Q 2 A/N 1	Y 28 F 1	Y 25 Q/L 1 T/E 1	E 15 D 14
General L-amino acid	22	P 22	L 22	F 22	Y 22	T 17 S/I 2 Q 1	D 22
Glu/Asp	47	P 46 M 1	L 47	F 46 N 1	Y 45 F 2	Q 46 E 1	D 47
His/Glu/Gln/Arg	25	P 25	V 10 L 9 I/F 3	N 22 F 3	Y 25	E 14 T 7 S 4	E 16 D 7 S/G 1

More than 50 amino acid transporters sharing high sequence identity with ArtQN were searched in the Kyoto Encyclopedia of Genes and Genomes (KEGG) database. Only the specified residues that are conserved in no fewer than 30 different transporters were considered and are summarized here.

Except for the maltose uptake system (13), no substrate binding sites within the TMDs of type I ABC importers have been identified. In the maltose transporter, substrate appeared in a large solvent-filled cavity in which stacking interactions by aromatic side chains and hydrogen bonds contribute to sugar recognition and binding (42). We have identified a previously unidentified recognition and binding mode in ArtQ. A negatively charged pocket located at the interface of two ArtQ subunits forms a polar amino acid-binding tunnel that allows positively charged substrates, such as Arg and His, to pass through. However, how substrates are eventually released from the binding pocket to the cytoplasm remains to be established. Based on the fact that its cognate SBP can only deliver one substrate molecule in each cycle, binding of two substrate molecules to the TMDs is quite unforeseen and warrants further investigation.

In summary, we have provided for the first time, to our knowledge, the structural basis of an amino acid-binding site within the TMD of an ABC importer. The observation that one substrate molecule is bound per subunit gives rise to the speculation that this might be a common feature of homodimeric type I ABC importers. Certainly, we need to await more structures of both heterodimeric and homodimeric transporters with bound substrates to prove this notion.

Methods

The artQ and artN genes were cloned from *T. tengcongensis* genomic DNA into a pACYCDuet vector (Novagen), which can coexpress ArtQ and ArtN stimultaneously using separate T7 promoters. An engineered C-terminal 6× His tag was fused to artQ. The artI gene was cloned from *T. tengcongensis* genomic DNA into a pet21b vector (Novagen) with a C-terminal 6× His tag. $Art(QN)_2$ complex and ArtI were purified from *E. coli* strains C43 and BL21, respectively. Crystals were grown at 18 °C by the hanging-drop vapor diffusion method. Diffraction data were collected at Shanghai Synchrotron Radiation Facility Beamline BL17U, and the structures were solved by molecular replacement. Data collection and structure refinement statistics are summarized in Table S1. For functional characterization, ArtI was subjected to a denaturation/renaturation procedure to remove prebound substrate as described previously (43). Incorporation of $Art(QN)_2$ variants into liposomes prepared from *G. stearothermophilus* total lipids was carried out, and ATPase activity was assayed essentially as described previously (26). More details are provided in *SI Methods*.

ACKNOWLEDGMENTS. We thank the staff at the Shanghai Synchrotron Radiation Facility Beamline BL17U for assisting with data collection and the China National Center for Protein Sciences Beijing for providing facility support. We also thank Dr. H. Tan (Institute of Microbiology, Chinese Academy of Sciences) for providing cells of *T. tengcongensis*. This work was supported by the Chinese Ministry of Science and Technology (Grants 2011CB910502 and 2012CB911101, to M.Y.), the National Natural Science Foundation of China (Grants 31030020 and 31170679, to M.Y.), and the Deutsche Forschungsgemeinschaft (PAK 459, Grant SCHN 274/14-2, to E.S.).

1. Higgins CF (1992) ABC transporters: From microorganisms to man. *Annu Rev Cell Biol* 8:67–113.
2. Holland IB, Blight MA (1999) ABC-ATPases, adaptable energy generators fuelling transmembrane movement of a variety of molecules in organisms from bacteria to humans. *J Mol Biol* 293(2):381–399.
3. Bouige P, Laurent D, Piloyan L, Dassa E (2002) Phylogenetic and functional classification of ATP-binding cassette (ABC) systems. *Curr Protein Pept Sci* 3(5):541–559.
4. Dean M, Hamon Y, Chimini G (2001) The human ATP-binding cassette (ABC) transporter superfamily. *J Lipid Res* 42(7):1007–1017.
5. Rees DC, Johnson E, Lewinson O (2009) ABC transporters: The power to change. *Nat Rev Mol Cell Biol* 10(3):218–227.
6. Ames GF (1986) Bacterial periplasmic transport systems: Structure, mechanism, and evolution. *Annu Rev Biochem* 55:397–425.
7. Gerber S, Comellas-Bigler M, Goetz BA, Locher KP (2008) Structural basis of trans-inhibition in a molybdate/tungstate ABC transporter. *Science* 321(5886):246–250.
8. Hvorup RN, et al. (2007) Asymmetry in the structure of the ABC transporter-binding protein complex BtuCD-BtuF. *Science* 317(5843):1387–1390.
9. Kadaba NS, Kaiser JT, Johnson E, Lee A, Rees DC (2008) The high-affinity *E. coli* methionine ABC transporter: Structure and allosteric regulation. *Science* 321(5886):250–253.
10. Khare D, Oldham ML, Orelle C, Davidson AL, Chen J (2009) Alternating access in maltose transporter mediated by rigid-body rotations. *Mol Cell* 33(4):528–536.
11. Hung LW, et al. (1998) Crystal structure of the ATP-binding subunit of an ABC transporter. *Nature* 396(6712):703–707.
12. Oldham ML, Chen J (2011) Crystal structure of the maltose transporter in a pre-translocation intermediate state. *Science* 332(6034):1202–1205.
13. Oldham ML, Khare D, Quiocho FA, Davidson AL, Chen J (2007) Crystal structure of a catalytic intermediate of the maltose transporter. *Nature* 450(7169):515–521.
14. Pinkett HW, Lee AT, Lum P, Locher KP, Rees DC (2007) An inward-facing conformation of a putative metal-chelate type ABC transporter. *Science* 315(5810):373–377.
15. Ward A, Reyes CL, Yu J, Roth CB, Chang G (2007) Flexibility in the ABC transporter MsbA: Alternating access with a twist. *Proc Natl Acad Sci USA* 104(48):19005–19010.
16. Lee JY, Yang JG, Zhitnitsky D, Lewinson O, Rees DC (2014) Structural basis for heavy metal detoxification by an Atm1-type ABC exporter. *Science* 343(6175):1133–1136.
17. Vasundara S, Antonio JP, Roland L (2014) Crystal structures of nucleotide-free and glutathione-bound mitochondrial ABC transporter Atm1. *Science* 343(1137):1136–1140.
18. Schneider E, Hunke S (1998) ATP-binding cassette (ABC) transport systems: Functional and structural aspects of the ATP-hydrolyzing subunits/domains. *FEMS Microbiol Rev* 22(1):1–20.
19. Walker JE, Saraste M, Runswick MJ, Gay NJ (1982) Distantly related sequences in the alpha- and beta-subunits of ATP synthase, myosin, kinases and other ATP-requiring enzymes and a common nucleotide binding fold. *EMBO J* 1(8):945–951.
20. ter Beek J, Guskov A, Slotboom DJ (2014) Structural diversity of ABC transporters. *J Gen Physiol* 143(4):419–435.
21. Oswald C, Holland IB, Schmitt L (2006) The motor domains of ABC transporters: What can structures tell us? *Naunyn Schmiedebergs Arch Pharmacol* 372(6):385–399.
22. Borths EL, Poolman B, Hvorup RN, Locher KP, Rees DC (2005) In vitro functional characterization of BtuCD-F, the *Escherichia coli* ABC transporter for vitamin B12 uptake. *Biochemistry* 44(49):16301–16309.
23. Davidson AL, Shuman HA, Nikaido H (1992) Mechanism of maltose transport in *Escherichia coli*: Transmembrane signaling by periplasmic binding proteins. *Proc Natl Acad Sci USA* 89(6):2360–2364.
24. Liu CE, Liu PQ, Ames GF (1997) Characterization of the adenosine triphosphatase activity of the periplasmic histidine permease, a traffic ATPase (ABC transporter). *J Biol Chem* 272(35):21883–21891.
25. Patzlaff JS, van der Heide T, Poolman B (2003) The ATP/substrate stoichiometry of the ATP-binding cassette (ABC) transporter OpuA. *J Biol Chem* 278(32):29546–29551.
26. Weidlich D, et al. (2013) Residues of a proposed gate region in type I ATP-binding cassette import systems are crucial for function as revealed by mutational analysis. *Biochim Biophys Acta* 1828(9):2164–2172.
27. Oldham ML, Chen J (2011) Snapshots of the maltose transporter during ATP hydrolysis. *Proc Natl Acad Sci USA* 108(37):15152–15156.
28. Bao H, Dalal K, Wang V, Rouiller I, Duong F (2013) The maltose ABC transporter: Action of membrane lipids on the transporter stability, coupling and ATPase activity. *Biochim Biophys Acta* 1828(8):1723–1730.
29. Heuveling J, et al. (2014) Conformational changes of the bacterial type I ATP-binding cassette importer HisQMP2 at distinct steps of the catalytic cycle. *Biochim Biophys Acta* 1838(1 Pt B):106–116.
30. Oh BH, et al. (1993) Three-dimensional structures of the periplasmic lysine/arginine/ornithine-binding protein with and without a ligand. *J Biol Chem* 268(15):11348–11355.
31. Vahedi-Faridi A, et al. (2008) Crystal structures and mutational analysis of the arginine-, lysine-, histidine-binding protein ArtJ from *Geobacillus stearothermophilus*: Implications for interactions of ArtJ with its cognate ATP-binding cassette transporter, Art(MP)2. *J Mol Biol* 375(2):448–459.
32. Oh BH, et al. (1994) The bacterial periplasmic histidine-binding protein: Structure/function analysis of the ligand-binding site and comparison with related proteins. *J Biol Chem* 269(6):4135–4143.
33. Sack JS, Saper MA, Quiocho FA (1989) Periplasmic binding protein structure and function: Refined X-ray structures of the leucine/isoleucine/valine-binding protein and its complex with leucine. *J Mol Biol* 206(1):171–191.
34. Locher KP (2009) Review: Structure and mechanism of ATP-binding cassette transporters. *Philos Trans R Soc Lond B Biol Sci* 364(1514):239–245.
35. Dassa E, Hofnung M (1985) Sequence of gene *malG* in *E. coli* K12: Homologies between integral membrane components from binding protein-dependent transport systems. *EMBO J* 4(9):2287–2293.
36. Saurin W, Köster W, Dassa E (1994) Bacterial binding protein-dependent permeases: Characterization of distinctive signatures for functionally related integral cytoplasmic membrane proteins. *Mol Microbiol* 12(6):993–1004.
37. Kelley LA, Sternberg MJ (2009) Protein structure prediction on the Web: A case study using the Phyre server. *Nat Protoc* 4(3):363–371.
38. Ames GFL, et al. (2001) Purification and characterization of the membrane-bound complex of an ABC transporter, the histidine permease. *J Bioenerg Biomembr* 33(2):79–92.
39. Liu PQ, Ames GFL (1998) In vitro disassembly and reassembly of an ABC transporter, the histidine permease. *Proc Natl Acad Sci USA* 95(7):3495–3500.
40. Locher KP, Lee AT, Rees DC (2002) The *E. coli* BtuCD structure: A framework for ABC transporter architecture and mechanism. *Science* 296(5570):1091–1098.
41. Newstead S, et al. (2009) Insights into how nucleotide-binding domains power ABC transport. *Structure* 17(9):1213–1222.
42. Oldham ML, Chen S, Chen J (2013) Structural basis for substrate specificity in the *Escherichia coli* maltose transport system. *Proc Natl Acad Sci USA* 110(45):18132–18137.
43. Hall JA, Davidson AL, Nikaido H (1998) Preparation and reconstitution of membrane-associated maltose transporter complex of *Escherichia coli*. *Methods Enzymol* 292:20–29.